Experimental Evidence for the Quantum Confinement Effect in 3*C*-SiC Nanocrystallites

X. L. Wu,[1,*,†] J. Y. Fan,[1,*] T. Qiu,[1] X. Yang,[1] G. G. Siu,[2] and Paul K. Chu[2]

[1]*National Laboratory of Solid State Microstructures & Department of Physics, Nanjing University, Nanjing 210093, People's Republic of China*

[2]*Department of Physics & Materials Science, City University of Hong Kong, Kowloon, Hong Kong, People's Republic of China*

(Received 15 July 2004; published 19 January 2005)

Using electrochemical etching of a polycrystalline 3*C*-SiC target and subsequent ultrasonic treatment in water solution, we have fabricated suspensions of 3*C*-SiC nanocrystallites that luminesce. Transmission electron microscope observations show that the 3*C*-SiC nanocrystallites, which uniformly disperse in water, have sizes in the range of 1–6 nm. Photoluminescence and photoluminescence excitation spectral examinations show clear evidence for the quantum confinement of 3*C*-SiC nanocrystallites with the emission band maximum ranging from 440 to 560 nm. Tunable, composite polystyrene/SiC film can be made by adding polystyrene to a toluene suspension of the 3*C*-SiC nanocrystallites and then coating the resulting solution onto a Si wafer.

DOI: 10.1103/PhysRevLett.94.026102 PACS numbers: 81.07.Bc, 78.55.Hx

Porous Si with room-temperature visible photoluminescence (PL) has been widely studied for 15 years [1,2]. Many models have been proposed to explain its PL mechanism, mainly including quantum confinement [3–5], surface states [6,7], and defect states [8,9]. So far, the commonly accepted theory is that the band gap is widened as a result of the quantum confinement of Si nanocrystallites, which pushes the PL peaks from the infrared to visible range for crystallite sizes below 5 nm [10,11]. For porous Si, a large number of investigations have indicated that it is very difficult to obtain strong and stable blue emission that is useful in optoelectronics. Therefore, based on porous Si luminescent mechanisms, many investigators have focused their attention on nanoscale SiC with robust structure and believe that its wide band gap (~ 2.2 eV for 3*C*-SiC) can more easily push the PL into the blue range [12–20]. So far, many efforts have been made, but the observed PL was generally beyond 550 nm (< 2.25 eV), which is connected with the amorphous fraction of the nanocrystallites and the surface chemical disorder induced by oxidation [21]. Explicit quantum confinement of nanoscale SiC has not yet been achieved experimentally due to the complexities in structure and sample preparation. Electrochemical etching of SiC single crystal failed in taking strong and blue PL because the formed crystallites are more than 20 nm in size [13]. Although several nanometer SiC crystallites have been achieved in some experiments [16–18,21], they were generally localized in a complicated matrix and have no obvious quantum confinement effect due to dominant surface-defect state features. Because of the lacks in experimental and theoretical information and the difficulties in sample preparation, the quantum confinement of SiC nanocrystallites has become a subject of many experimental and theoretical investigations.

In this Letter, we report experimental evidence for the quantum confinement effect in 3*C*-SiC, exhibited through nanocrystallites with sizes almost continuously ranging from 1 to 6 nm. The samples are the suspensions of fine 3*C*-SiC nanocrystallites, which were obtained through two steps. First, we used highly catalyzed electrochemical etching of polycrystalline 3*C*-SiC wafer in HF-ethanol ($HF : C_2H_5OH = 2:1$) solution under illumination with a 150 W halogen lamp from a distance of 15 cm to obtain porous SiC (PSC). The anodic time was 60 min and the etching current densities were 100, 70, 60, 40, and 20 mA/cm^2, respectively. Each PSC was then transferred to an ultrasound water (or toluene) bath, in which the top porous structure film was crumbled into small nanocrystallites dispersed in the solvent [22,23]. Secondly, each porous sample was again etched in HF-ethanol at the current density of 20 mA/cm^2 for 1 h, followed by further treatment in the ultrasonic water (or toluene) bath. This process was repeated but with the current densities of 40 and 60 mA/cm^2, respectively. Now small nanocrystallites were almost completely separated from the porous structure to form a suspension of SiC nanocrystallites. We name the suspensions with SiC nanocrystallites from the PSC samples initially formed at etching current densities of 100, 70, 60, 40, and 20 mA/cm^2 as samples A, B, C, D, and E, respectively. Finally surplus PSC sample was etched at a current density of 100 mA/cm^2 for 1 h and then treated in the ultrasonic water (toluene) bath, by which the obtained suspension only contains large nanocrystallites. To make a solid film, we added polystyrene to a toluene suspension with the 3*C*-SiC nanocrystallites and then coated the resulting solution onto a Si wafer.

Figure 1(a) shows a transmission electron microscopy (TEM) image of the nanocrystallites from sample C, taken by dripping the suspension on a graphite grid. It can be seen that the nanocrystallites are almost spherical, with diameters ranging from 1 to 6 nm. The lattice fringes corresponding to the {111} plane of 3*C*-SiC can clearly be observed from the high-resolution TEM image of the

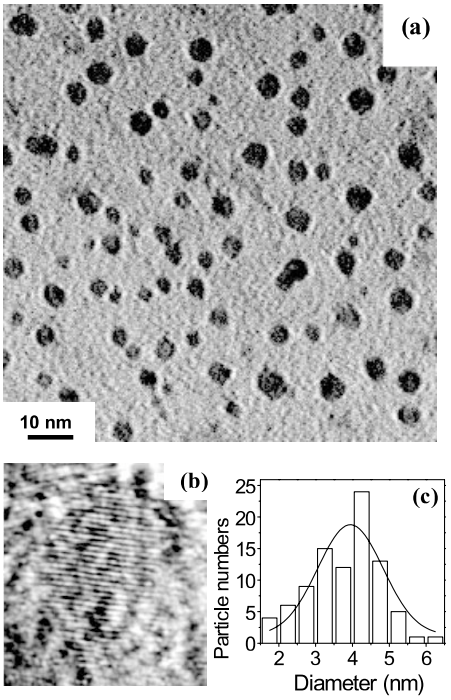

FIG. 1. (a) TEM image of sample C. The nanocrystallites are nearly spherical. (b) HRTEM image of one nanoparticle. The lattice fringes corresponding to the {111} plane of 3*C*-SiC can clearly be identified. (c) The particle number distribution with a center size of 3.9 nm, which was obtained using a Gaussian fitting.

crystallites [see Fig. 1(b)]. The particle size distribution is depicted in Fig. 1(c), which shows an asymptotic centric distribution. A Gaussian fitting indicates that the maximal probability for crystallite diameter is 3.9 nm. For samples B, D, and E, our TEM observations show that their crystallite size distributions are similar to that in sample C. For sample A, we found that the crystallite concentration is relatively low in comparison with those of samples B, D, C, and E. Its crystallite size distribution is in the range of 6–10 nm, having a maximal probability of 8.8 nm in crystallite diameter.

Since the nanocrystallites are almost continuously distributed with a center size of 3.9 nm, the PL peak from the suspensions should redshift as the excitation wavelength increases according to the quantum confinement effect. This is verified by measuring the room-temperature PL spectra under excitation with different wavelengths ranging from 240 to 500 nm [see Fig. 2(a), taken from sample D]. Figure 2(b) more clearly shows this result, where the PL peak position is depicted as a function of the excitation wavelength. For samples B, C, D, and E, from the beginning of the 320 nm excitation line, the PL band maximum always increases with the excitation wavelength, finally reaching about 540 nm under excitation with the 500 nm line. As the excitation wavelength is more than 500 nm, no noticeable emission was observed. For sample A with large nanocrystallites (> 6 nm), the intensity of the emission band is enhanced as a result of the decrease of crystallite sizes, because bulk 3*C*-SiC only has a low blue emission at low temperatures [24]. However, we can see that the peak position of the emission remains at $\sim$550 nm (2.25 eV), just being the band gap of bulk 3*C*-SiC [16,25]. The PL behavior of sample A is different from those of other samples, but also shows a band-to-band recombination feature. Figure 2(c) shows the Stokes shift versus the excitation wavelength. One can see that with increasing the excitation wavelength, the Stokes shift gradually approaches zero. For sample A, this process is more pronounced. Its Stokes shift linearly trends to zero with increasing excitation wavelength, indicating the existence of the band gap of bulk 3*C*-SiC, which is in good agreement with the data reported in Ref. [25]. The PL intensity versus the excitation wavelength is shown in Fig. 2(d), where a centric distribution of maximal PL intensity can clearly be observed. This result further demonstrates the size distribution of the nanocrystallites to be very consistent with that shown in Fig. 1(c). From Fig. 2(d), we can also see that the PL intensity of sample A is relatively low. Two factors can lead to the situation. One is due to its low crystallite concentration. The other is because it has large crystallite sizes, which result in low excitation efficiency. Here we should mention that the fixed small peak in every spectrum of Fig. 2(d) is due to a slight leakage of the strong 467 nm light of the Xe lamp, which mixes in all the excitation light.

We also performed the PL detection of the as-etched porous 3*C*-SiC samples before they were treated in an ultrasonic water bath, but no similar emission was obtained. This result is consistent with that obtained from electrochemical etching of 6*H*-SiC [13]. It is understandable because the nanocrystallites in the as-etched samples are interweaved with each other. After ultrasonic treatment, they become individual nanocrystallites, which exhibit the quantum confinement effect. We found that the solid film synthesized by adding polystyrene to a toluene suspension of the 3*C*-SiC nanocrystallites and then coating the resulting solution onto a Si wafer mainly has emissions in the blue [see Fig. 2(a)]. The obtained PL is rather stable not only in peak position but also in peak intensity, indicating that the SiC nanocrystallite film is excellent as light-emitting nanomaterial.

The emission intensities from the suspensions of 3*C*-SiC nanocrystallites are far greater than those from porous silicon samples or the suspensions of Si nanocrystallites with the same sizes [22]. The emission spots are visible with the naked eye only under excitation with an Xe lamp. Figure 3 shows three typical emission photos, which were taken using a Canon digital camera. The suspension containing the 3*C*-SiC nanocrystallites was placed in a rectangular glass container. Under excitation with three different wavelengths, 320, 400, and 450 nm, the emission

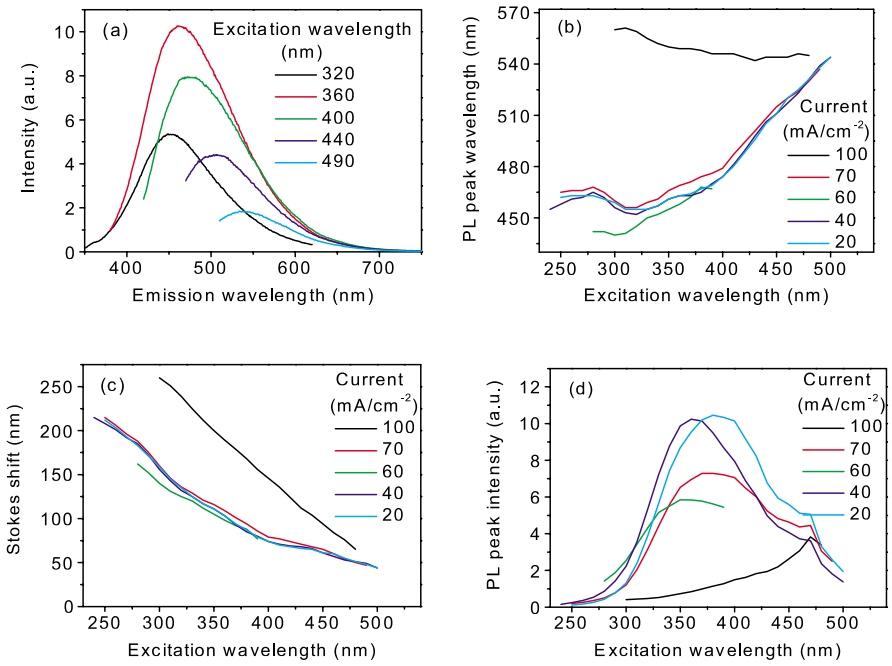

FIG. 2 (color). (a) PL spectra of sample D, taken under five different excitation wavelengths ranging from 320 to 490 nm. (b) PL peak position versus the excitation wavelength for samples A, B, C, D, and E. (c) The Stokes shift versus the excitation wavelength for samples A, B, C, D, and E. (d) PL peak intensity versus the excitation wavelength for samples A, B, C, D, and E.

spots are seen to be blue (~ 450 nm), blue-green (~ 510 nm), and green-yellow (~ 545 nm) (from left to right), respectively. For taking the pictures, we used a filter of 488 nm to avoid the strong blue background scattering of the container caused by the leakage of the 467 nm light of the Xe lamp when the excitation wavelength is close to 467 nm.

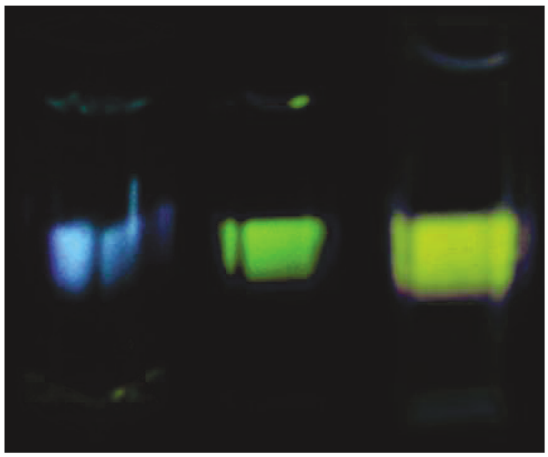

FIG. 3 (color). Emission photos from samples D (two of the left side) and A (the right side) under excitation with three different wavelengths, 320, 400, and 450 nm. The emission wavelengths can be identified to be blue (~ 450 nm), blue-green (~ 510 nm), and green-yellow (~ 545 nm) (from left to right), respectively.

For semiconductor nanomaterials, some theoretical models have been developed dealing with the band gap widening by quantum confinements [20] and surface reconstructions [21]. To theoretically identify the origin of the observed emissions, we first estimate the Bohr radius R of 3C-SiC and then obtain the increase in the band gap energy as the crystallite sizes d decrease to 3.9 nm. For 3C-SiC, the longitudinal and transverse effective masses of electron $m_l = 0.647m_0$, $m_t = 0.24m_0$ and the effective masses of heavy and light hole $m_h(h) = 1.2m_0$, $m_h(l) = 0.125m_0$ [26]. As an approximate calculation, we take the effective mass of electron $m_e = (m_l m_t)^{1/2} = 0.394m_0$ and that of hole $m_h = [m_h(l)m_h(h)]^{1/2} = 0.387m_0$. The Bohr radius R can be written as $R = \epsilon(m_0/\mu)a_0$ [27], where $\mu = m_e m_h/(m_e + m_h)$ is the reduced mass of the exciton, $\epsilon \cong 10$ the high-frequency dielectric constant of 3C-SiC, and $a_0 = 0.053$ nm. Thus, R can be obtained to be 2.7 nm. The R value meets $d/R < 2$, so such nanocrystallites with size of 3.9 nm are of obvious quantum confinement effect (electron-hole confinement [28]). Under the effective-mass approximation, the size dependence of the band gap can be represented as follows [29,30]: $E^* = E_g + h^2/8\mu r^2 - 1.8e^2/4\pi\epsilon_o\epsilon r$, where $E_g = 2.2$ eV is the band gap of bulk material and $r = d/2$. For the nanocrystallites with sizes of $d = 3.9$ nm, we can estimate E^* to be $\sim$2.7 eV (~ 460 nm), which is in excellent agreement with our observation. For sample D with the crystallite size of 8.8 nm, E^* is equal to $\sim$2.3 eV (~ 540 nm), just being the band gap of bulk 3C-SiC. The above theoretical calcu-

lations further indicate that not only the quantum confinement exists for the current 3*C*-SiC nanocrystallites but also the observed emissions really arise from the band-to-band recombination of photoexcited carriers in the quantum confined 3*C*-SiC nanocrystallites.

In conclusion, to our knowledge, this is the first explicit observation of the quantum confinement effect of SiC nanocrystallites, since the investigations on the PL mechanism of SiC nanocrystallites starting from around mid 1990s [12–16]. The emission can be continuously tuned in a range from 440 to 560 nm, together with the superiority of strong luminescence and stability, pointing to a new way for applications in nanoelectronics and optoelectronics.

This work was supported by the National Natural Science Foundations of China (Project Nos. 10225416, 60178036, and 60476038) and the LPEMST as well as the special funds for Major State Basic Research Project No. G001CB3095 of China. Partial support was also provide by Hong Kong Research Grants Council (RGC) Competitive Earmarked Research Grant (CERG) No. CityU 1137/03E and City University of Hong Kong Strategic Research Grant No. 7001642.

*Corresponding author
†Electronic address: hkxlwu@nju.edu.cn

[1] A. Fowler, Phys. Today **50**, 50 (1997).
[2] K. D. Hirschman, L. Tsybeskov, S. P. Duttagupta, and P. M. Fauchet, Nature (London) **384**, 338 (1996).
[3] L T. Canham, Appl. Phys. Lett. **57**, 1046 (1990).
[4] V. Lehman and U. Gösele, Appl. Phys. Lett. **58**, 856 (1991).
[5] J. P. Proot, C. Delerue, and G. Allan, Appl. Phys. Lett. **61**, 1948 (1992).
[6] F. Koch, V. Petrova-Koch, and T. Muschik, J. Lumin. **57**, 271 (1993).
[7] Y. Kanemitsu, H. Uto, and Y. Masumoto, Phys. Rev. B **48**, 2827 (1993).
[8] S. M. Prokes, Appl. Phys. Lett. **62**, 3244 (1990).
[9] X. L. Wu *et al.*, Phys. Rev. Lett. **91**, 157402 (2003).
[10] M. V. Wolkin, J. Jorne, P. M. Fauchet, G. Allan, and C. Delerue, Phys. Rev. Lett. **82**, 197 (1999).
[11] X. L. Wu *et al.*, Phys. Rev. B **62**, R7759 (2000).
[12] A. O. Konstantinov, C. I. Harris, and E. Janzén, Appl. Phys. Lett. **65**, 2699 (1994).
[13] V. Petrova-Koch *et al.*, Thin Solid Films **255**, 107 (1995).
[14] J. S. Shor *et al.*, J. Appl. Phys. **76**, 4045 (1994).
[15] T. Matsumoto *et al.*, Appl. Phys. Lett. **64**, 226 (1994).
[16] L. S. Liao, X. M. Bao, Z. F. Yang, and N. B. Min, Appl. Phys. Lett. **66**, 2382 (1995).
[17] X. L. Wu *et al.*, Appl. Phys. Lett. **77**, 1292 (2000).
[18] X. L. Wu *et al.*, J. Appl. Phys. **94**, 5247 (2003).
[19] L. Tilgman *et al.*, J. Appl. Phys. **95**, 490 (2003).
[20] D. H. Feng *et al.*, Phys. Rev. B **68**, 035334 (2003).
[21] A. Kassiba *et al.*, Phys. Rev. B **66**, 155317 (2002).
[22] J. Heinrich *et al.*, Science **255**, 66 (1992).
[23] M. Nayfeh *et al.*, Appl. Phys. Lett. **75**, 4112 (1999).
[24] M. Ikeda, H. Matsunami, and T. Tanaka, Phys. Rev. B **22**, 2842 (1980).
[25] J. R. Q'Connor and J. Smiltens, *Silicon Carbide* (Pergamon, London, 1960).
[26] N. W. Jepps and T. F. Page, in *Crystal Growth and Characterization*, edited by P. Krishna (Pergamon, New York, 1983), Vol. 7.
[27] J. P. Wolfe, Phys. Today **35**, 46 (1982).
[28] R. Reisfeld, J. Alloys Compd. **341**, 56 (2002).
[29] L. Brus, J. Phys. Chem. **90**, 2555 (1986).
[30] X. L. Wu, G. G. Siu, C. L. Fu, and H. C. Ong, Appl. Phys. Lett. **78**, 2285 (2001).